ARTICLE

임계열유속 향상을 위한 나노물질의 산화처리에 대한 연구

김우중* · 전용한** · 김남진***†

*한국전기차정비협동조합
**상지영서대학교 소방안전과
***제주대학교 에너지공학과

Study on the Oxidation Treatment of Nanoparticles for the Critical Heat Flux

Woo-Joong Kim* · Yong-Han Jeon** · Nam-Jin Kim***†

*Korea Electric Vehicle Maintenance Cooperative
**Department of Fire and Frotection, Sangji-Youngseo College
***Department of Nuclear & Energy Engineering, Jeju National Univ.

†Corresponding author: jnkim@jejunu.ac.kr

Abstract

Pool boiling, one of the key thermal-hydraulics phenomena, has been widely studied for improving heat transfer efficiencies and safety of nuclear power plants, refrigerating systems, solar-collector heat pipes, and other facilities and equipments. In the present study, the critical heat flux (CHF) and heat-transfer coefficients were tested under the pool-boiling state using graphene M-5 and M-15 nanofluids as well as oxidized graphene M-5 nanofluid. The results showed that the highest CHF increase for both graphene M-5 and M-15 was at the 0.01% volume fraction and, moreover, that the CHF-increase ratio for small-diameter graphene M-5 was higher than that for large-diameter graphene M-15. Also at the 0.01% volume fraction, the oxidized graphene M-5 nanofluid showed a 41.82%-higher CHF-increase ratio and a 26.7%-higher heat-transfer coefficient relative to the same nanofluid without oxidation treatment at the excess temperature where the CHF of distilled water occurs.

Keywords: 열전달(Heat transfer), 비등(Boiling), 그래핀(Graphene), 산화(Oxidation), 임계열유속(Critical heat flux)

Journal of the Korean Solar Energy Society
Vol.37, No.6, pp.39-49, December 2017
https://doi.org/10.7836/kses.2017.37.6.039

pISSN : 1598-6411

eISSN : 2508-3562

Received: 23 August 2017

Revised: 13 December 2017

Accepted: 29 December 2017

1. 서 론

Nucleate boiling is one of the most important phenomena in various industries and devices such as power generations, heat exchangers, high-power electronic component cooling, and solar-collector heat pipes. Critical heat flux (CHF) refers to the upper limit of the pool-boiling heat-transfer region. Whereas, before the CHF happens, the heat-transfer coefficient is high enough to attain a sufficiently high heat

flux at a relatively low surface heat, beyond the CHF, vapor bubbles on the heating surface start to combine, forming a vapor film that greatly reduces th e heat-transfer rate between the heating surface and the liquid[1]. After the CHF, the heat-transfer coefficient markedly decreases with the heating surface temperature of the heat-transfer apparatus, concomitantly, is greatly increased. This incurs a risk of physical failure of the heat-transfer apparatus. Therefore, for both economic efficiency and the safety of the heat-transfer apparatus, it is vital to increase the CHF.

Many researchers have found that the CHF can be significantly increased by addition of tiny amounts of nanometer-size particles, known as nano particles, for conventional cooling liquids. Such nanofluids dispersed in a base liquid, as heat-transfer agents, have been studied in various fields of thermal engineering[2]. Bang and Chang (2005) confirmed a CHF increaseas high as 32% in Al_2O_3 nanofluid compared with base fluid[3]. Park and Jung (2009), tested ing the application of carbon nanotubes in nanofluid formulation using R-22 as a coolant, noted an approximately 30% heat-transfer-coefficient increase in the low heat flux section at 100 kW/m^2 or less[4]. Liu and Liao (2008), have carried out tests on nanofluid formulated by adding CuO and SiO_2 to water and C_2H_5OH, found that with the volume fraction of 0.01%, there could be no effect on the heat-transfer coefficient[5]. Golubovic et al. (2009) reported 50 and 30% CHF increases with Al_2O_3 and Bi_2O_3 nanofluids, respectively[6,7]. Phan et al. (2009) carried out a pool-boiling experiment on specimens coated with SiOx, TiO_2, Pt, Fe_2O_3, SiOC, and Teflon, and reported that the contact angle and bubble-departure diameter had significant effects on the heat-transfer coefficient[8]. Soltanietal et al. (2010) noted in the results of a test using a nanofluid formulated by diffusing Al_2O_3 nanoparticles in Carboxy Methyl Cellulose (CMC) solution that the heat-transfer coefficient had decreased in the high-concentration CMC solution but had increased by about 25% in a nanofluid mixture of nanoparticles and CMC solution[9]. Truong et al.(2010), for the purposes of a CHF experiment, fabricated a plate heater coated by a sandblast method with diamond, zinc oxide, and alumina nanofluids[10], while Ahn et al. (2010, 2013) conducted a pool-boiling CHF experiment involving anodization coating on a Zircaloy-4 surface using a plate heater[11,12]. The latter also carried out the same experiment using an Ni-Cr wire heater coated with 0.0005 wt.%-reduced graphene oxide, and confirmed that as the coating time increased, the CHF increased also. Most of the studies employing metallic nano-materials have reported problems such as heating-surface deposition and low nanofluid dispersibility. Phan et al. (2009) carried out a pool-boiling experiment on specimens coated with SiOx, TiO_2, Pt, Fe_2O_3, SiOC, and Teflon. It was reported that the contact angle and the bubble departure diameter had effects on the heat-transfer coefficient[13], and Yu et al. (2011) found that the thermal conductivity of ethylene glycol (EG)-based graphene nanofluid was increased 86% in a 5.0

vol% mix ratio[14].

In this context, graphene, boasting a higher thermal conductivity than any other nanoparticles, has been attracting at tention as a new heat-transfer material[15]. Therefore, in this study, in an effort to resolve issues related to nano-material heating-surface deposition and low dispersibility, CHF and heat-transfer coefficients were measured in the pool-boiling state through the oxidation treatment of graphene.

2. Experimental Apparatus and Method

2.1 Experimental apparatus

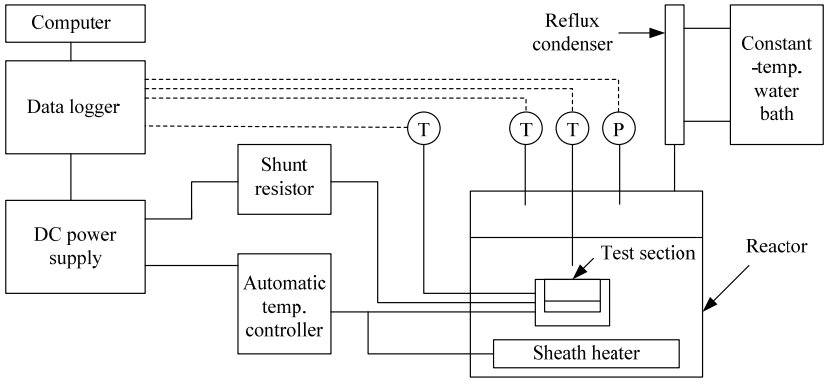

Fig. 1 Schematic diagram of CHF experimental apparatus

Table 1 Properties of graphenes M-5 and M-15

Properties	M-5	M-15
Diameter (nm)	5	15
Thickness (nm)	6-8	6-8
Purity (wt.%)	99.5	99.5
Bulk Density (g/cm^3)	0.03-0.1	0.03-0.1
True Density (g/cm^3)	2.2	2.2
Thermal Conductivity (W/m·K)	3,000	3,000
Surface Area (m^2/g)	120-150	120-150

Fig. 1 is a schematic diagram of the apparatus used in this experiment. The stainless steel alloy (SUS 316)-encased reactor, which generates heat flux for the pool-boiling state, and an automatic temperature controller regulates the temperature inside the reactor. Observation of the CHF phenomenon is made possible through quartz windows of 45 mm thickness installed in the front and back of the reactor. A reflux distiller for collection of evaporated vapor, installed at the top of the reactor, is connected to a chiller that

condenses the vapor for its return to the reactor. A pressure sensor of ±0.8% error and two T-type thermocouples of ±0.1℃ error are installed at the top and middle levels of the reactor, respectively, for measurement of pressure and temperature. A sheath heater of 8 mm diameter is installed at the lower level of the reactor to maintain the experimental pressure and temperature. The heat-transfer test section (37 mm × 40 mm × 30 mm) used in this experiment is composed of a zirconium (9.53 mm × 9.53 mm × 4mm). As the test section heat source, a 25 Ω heat-resistor heater (9.53 mm × 9.53 × 2.00 mm, CCR-375-1, Component General Inc.) was used. The heat-resistor heater had a 350 W maximum heat generation capacity that when combined with the zirconium specimen, a 3850 kW/m^2 maximum heat flux generation capability. The zirconium specimen had three evenly spaced holes of 1 mm diameter and 4.8 mm depth, into which T-type thermocouples were inserted for temperature measurement of zirconium specimen surface. In order to isolate heat generated from the heat-resistor heater as much as possible and to supply heat only to the zirconium specimen, the heat-transfer test section for the pool-boiling heat-transfer experimentation was made of PEEK, which has a very low heat-transfer rate. A DC power supply (DAP-125, Dau Nanotek) was used to supply electric power to the pool-boiling heat-transfer test section with generated heat flux to allow for increase of the voltage and current to 125 V and 8 A, respectively (maximum : 750 W). Additionally, in order to measure the heat quantity supplied to the test section, specifically the supplied current and voltage drop, a shunt resistor (221509, Yokogawa Co.) was installed between the DC power supply and the test section. For prevention of damage to the heat-resistor at the moment of CHF occurrence from the rapid heat transfer test section temperature increase, an automatic temperature controller (NX9, Hanyoung nux) was installed to automatically disconnect the DC power supply once the temperature exceeded 155℃. A data logger (34970a, Agilent) and a computer were set up to collect and store the measured data, and a CHF measuring program was written for real-time monitoring and effective processing of the data using Labview. In this study, graphene fabricated by Chemical Vapor Deposition was used. Using graphene nanoplatelets grade M, graphene nanofluids were synthesized by sonication. The physical properties of both graphene M-5 and M-15 nanoplatelets are listed in Table 1. As indicated, they are of high thermal conductivity and purity.

2.2 Experimental method

For CHF investigation and measurement, the reactor was filled with distilled water, and a vacuum pump was used to set the experimental pressure (19.61 kPa). After confirming that the pressure of the reactor was maintained at the experimental pressure, the temperature of the distilled water was increased to the target

temperature (60℃) using the sheath heater. Then, the DC power supply was connected, heating the test section in increments of 10 kW/m^2 to a level sufficient for generation of heat flux. Subsequently the CHF was calculated according to convection heat-transfer Eq.(1), and the pool-boiling heat-transfer coefficient on the specimen surface along with the quantity of heat were calculated by Eqs. (2) and (3), respectively, as

$$q'' = h(T_{wall} - T_{sat}) \tag{1}$$

$$h = \frac{Q/A}{(T_{wall} - T_{sat})} \tag{2}$$

$$Q = IV \tag{3}$$

where A is the heat-transfer area (m^2), I is the current capacity (A), Q is the supplied heat quantity (W), Tsat is the saturated temperature of distilled water (K), V is the voltage drop (V), h is the pool-boiling heat-transfer coefficient (kW/m^2·K), and q″ is the heat flux (kW/m^2). In this case, the zirconium surface temperatures were averaged from the values measured by the three inserted T-type thermocouples. The actual zirconium specimen surface temperatures Twall were calculated by incorporating the measured average temperature Tave into the linear heat-transfer equation

$$T_{wall} = T_{ave} - \frac{Q}{A}\left(\frac{l}{k}\right) \tag{4}$$

where, l is the distance from the inserted thermocouple to the surface (m) and k is the heat-transfer rate of the specimen (W/m·K)

3. Experimental Results and Discussion

3.1 Uncertainty

An analysis of the uncertainty of the data obtained in the CHF experiment in distilled water was carried out using the error propagation method of Kline and McClintock (1953)[16]. Heat flux and heat-transfer coefficient Equations are shown in Eq. (1) ~ (3), it can be seen that the heat flux factors are the heat-transfer coefficient and the difference between the zirconium specimen surface temperature and the

working fluid temperature. The heat-transfer coefficient factors are the current, voltage drop, specimen area, specimen surface temperature, and working fluid temperature. Therefore, the heat flux and the heat-transfer coefficient can be expressed with the functions.

$$q'' = q''(h, T_{wall} - T_{sat}) \tag{8}$$

$$h = h(I, V, L, T_{wall}, T_{sat}) \tag{9}$$

And, according to which factor, the equations for calculation of the uncertainty of the heat flux and heat-transfer coefficient results, respectively, are as follows:

$$\frac{U_{q''}}{q''} = \sqrt{\left(\frac{U_h}{h}\right)^2 + \left(\frac{U_{T_{wall} - T_{sat}}}{T_{wall} - T_{sat}}\right)^2} \tag{10}$$

$$\frac{U_h}{h} = \sqrt{\left(\frac{U_I}{I}\right)^2 + \left(\frac{U_V}{V}\right)^2 + \left(\frac{U_L}{L}\right)^2 + \left(\frac{U_{T_{wall}}}{T_{wall}}\right)^2 + \left(\frac{U_{T_{sat}}}{T_{sat}}\right)^2} \tag{11}$$

where $U_{q''}, U_h, U_{T_{wall} - T_{sat}}, U_I, U_V, U_L, U_{T_{wall}}$ and $U_{T_{sat}}$ are the uncertainties of the CHF, pool-boiling heat transfer coefficient, temperature difference between specimen and working fluid temperature, current, voltage drop, specimen length, specimen surface temperature, and working fluid temperature, respectively. As calculated from these equations, the uncertainties of the CHF and pool-boiling heat-transfer coefficients were $\pm 2.2\%$ and $\pm 6.7\%$, respectively, for every fluid carried out in the study.

3.2 CHF and pool-boiling heat-transfer coefficients of graphene

Fig. 2(a) provides comparative plots of the CHFs of the graphene M-15 nanofluid and distilled water. As can be seen, the CHF as measured at the nanofluid volume fractions of 0.0001, 0.001, 0.01, and 0.1% attained the increased values of 45.45, 76.36, 129.09, and 50.90%, respectively, compared with those measured with distilled water. Clearly, these results reflected the effect of the nanofluids' suppression of vapor formation. Indeed, without the nanofluids, the vapors would have obstructed the heat transfer on the zirconium specimen surface, or prevented the small vapors from aggregating to form larger ones. However,

the CHF value at the 0.1% volume fraction was lower than that at 0.01%. This indicated that the nanofluid's volume fraction was too large, meaning that nanoparticles obstructed the transfer of distilled water between the zirconium specimen and the vapors when pool boiling occurred on the zirconium surface. Based on the results, the optimal volume fraction for enhanced CHF was determined to be 0.01%. Fig. 2(b) provides comparative plots of the pool-boiling heat-transfer coefficients of graphene M-15 nanofluid and distilled water to the point of the CHF. As shown above, both fluids increased proportionally with the increased of heat flux. The pool-boiling heat-transfer coefficients of graphene M-15 nanofluid for the 0.0001, 0.001, and 0.01% volume fractions were increased relatively to that of distilled water at the excess temperature (Twall-Tsat) by 3.05, 9.09, and 16.00%, respectively. However, for the 0.1% volume fraction, it was decreased by 0.30%.

Fig. 3(a) shows comparative plots of the CHFs of the graphene M-5 nanofluid and the distilled water cases. As shown in the figure, the CHF measured at the 0.0001, 0.001, 0.01, and 0.1% volume fractions attained enhanced values of 52.73, 87.27, 145.45, and 70.01%, respectively, relative to those measured with distilled water. For the graphene M-15 nanofluid, the optimal volume fraction for enhanced CHF was determined as 0.01%. Fig. 3(b) shows comparative plots of the heat-transfer coefficients of graphene M-5 nanofluid and the distilled water to the point of the CHF. As indicated in the figure, the CHF of both fluids increased proportionally with the increas of heat flux. The heat-transfer coefficients of the graphene M-5 nanofluid for the 0.0001, 0.001, 0.01, and 0.1% volume fractions were increased by 6.25, 12.51, 22.05, and 1.36%, respectively, relative to those of distilled water at the excess temperature. Contrary to the case of graphene M-15, the pool-boiling heat-transfer coefficient at the volume fraction of 0.1% showed only a small increase.

As shown in Fig. 4(a), in the case of every volume fraction, the ratio for the large-diameter graphene M-5 nanofluid was higher than that for the small-diameter graphene M-15 nanofluid. Whereas both nanofluids showed the highest CHF increase with the 0.01% volume fraction, where that of graphene M-5 was 16.36% higher than that of graphene M-15. Also, as indicated in Fig. 4(b), the heat-transfer-coefficient increase ratio for the graphene M-5 nanofluid was 9.0% higher than that for the graphene M-15 nanofluid at the 0.01% volume fraction.

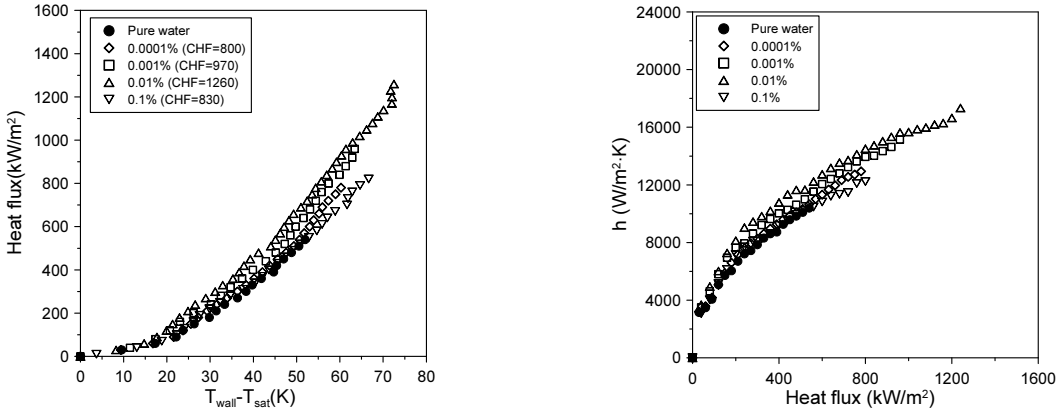

Fig. 2 Graphene M-15

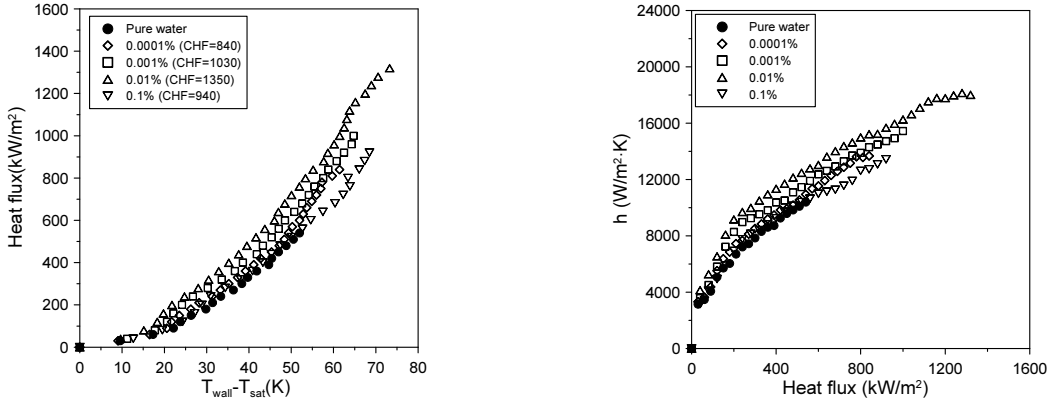

Fig. 3 Graphene M-5

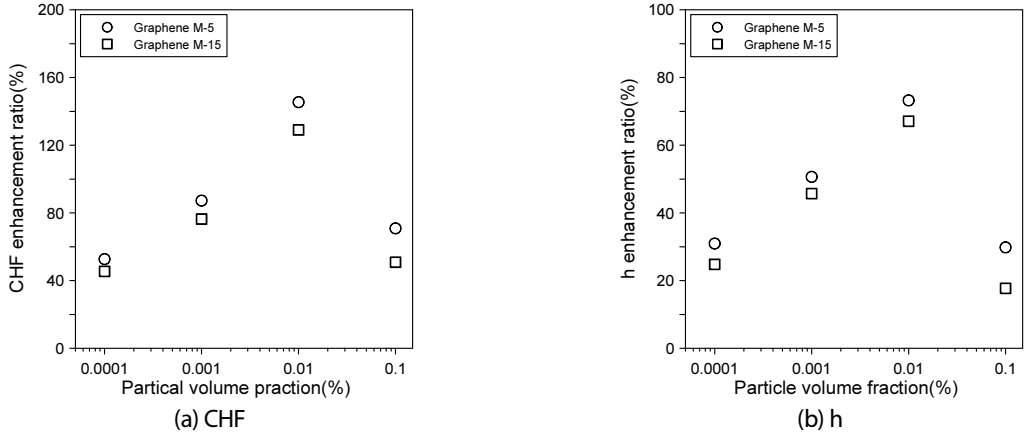

Fig. 4 Comparison of critical heat fluxs and pool-boiling heat-transfer coefficients enhancement ratios

3.2 CHF and pool-boiling heat-transfer coefficient of oxidized grapheme

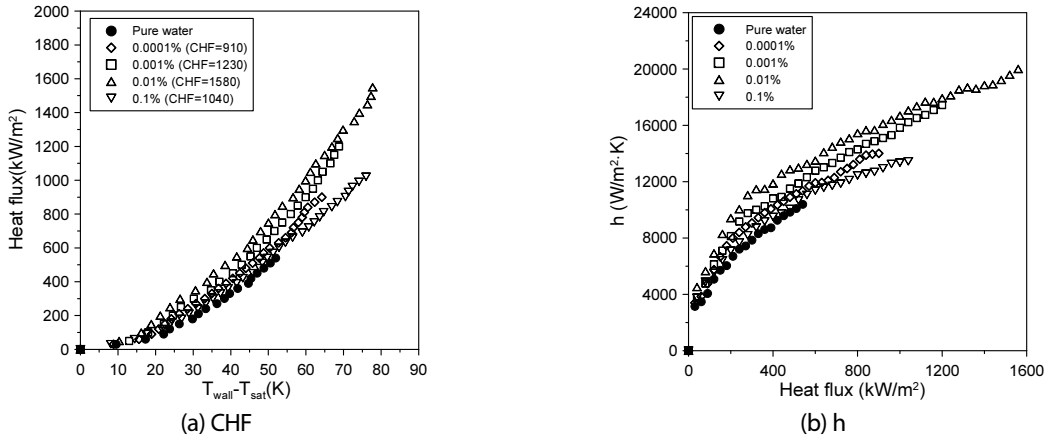

Fig. 5 Critical heat fluxs and pool-boiling heat-transfer coefficients of oxidized graphene M-5

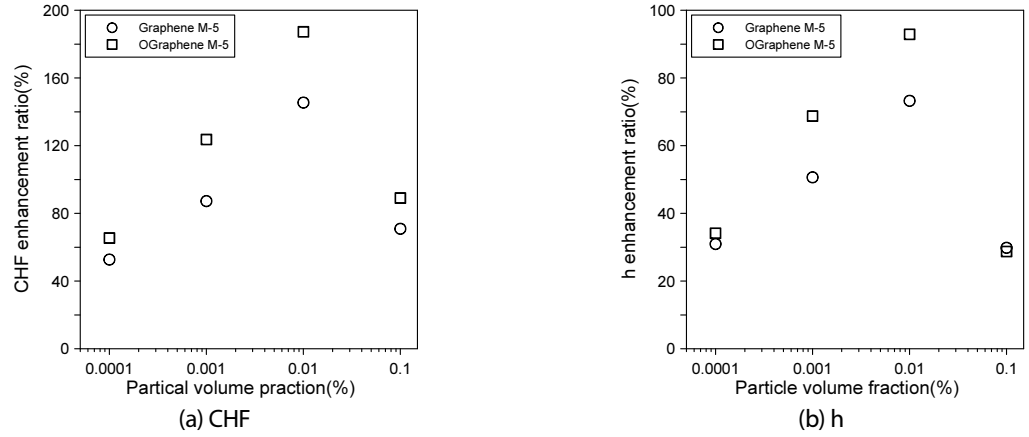

Fig. 6 Comparison of critical heat fluxs and pool-boiling heat-transfer coefficients enhancement ratios

Fig. 5(a) plots the comparative CHFs of the oxidized graphene M-5 nanofluid and the distilled water. As shown in the above figures, the CHF measured at the 0.0001, 0.001, 0.01, and 0.1% volume fractions could attain the increased values of 64.45, 123.63, 187.27, and 89.09% respectively. From these results, the optimal volume fraction for enhancing CHF was determined as 0.01%. Also, the CHF curve of the oxidized and non-oxidized graphene M-5 nanofluids similar with the volume fraction of 0.1%. Also, the pool-boiling heat-transfer coefficients of the oxidized graphene M-5 nanofluid and distilled water to the point of the CHF are shown in Fig. 5(b). From these results, the pool-boiling heat-transfer coefficients of the nanofluid for the 0.0001, 0.001, 0.01, and 0.1% volume fractions were increased by 9.93, 16.44, 26.67, and 4.99%, respectively, relative to those of distilled water at the excess temperature.

Fig. 6(a) compares the CHF-increase ratios of the oxidized graphene M-5 nanofluid and non-oxidized

graphene M-5 nanofluid relative to the CHF of distilled water. As shown in the figure, at every volume fraction, the ratio for the oxidized graphene M-5 nanofluid was higher. Notably, at the 0.01% volume fraction, the CHF-increase ratio of the oxidized graphene M-5 nanofluid was 41.82% higher than that of the graphene M-5 nanofluid without oxidation treatment. Also, Fig. 6(b) compares the pool-boiling heat-transfer-coefficient increase ratios for the oxidized graphene M-5 nanofluid and the non-oxidized graphene M-5 nanofluid relative to the pool-boiling heat-transfer coefficient of distilled water at the excess temperature where the CHF of distilled water occurred. As indicated above, the pool-boiling heat-transfer-coefficient increase ratio for the oxidized graphene M-5 nanofluid was 26.7% higher at the volume fraction of 0.01%.

4. Conclusion

In the current results, both graphene M-5 and M-15 nanofluids showed the highest CHF-increase ratio at the 0.01% volume fraction. At this volume fraction, that of the graphene M-5 nanofluid was about 16.36% higher than that of the graphene M-15 nanofluid. Meanwhile, the pool-boiling heat-transfer-coefficient increase ratio of the oxidized graphene M-5 nanofluid was 9.0% higher than that of graphene M-15 nanofluid without oxidation treatment. Also, the oxidized graphene M-5 nanofluid showed a 41.82%-higher CHF-increase ratio and a 26.7%-higher heat-transfer coefficient relative to non-oxidized graphene M-5 nanofluid. Moreover, the oxidized graphene M-5 nanofluid showed a better dispersibility performance and degree of deposition. Overall, the results served to highlight the effectiveness of graphene M-5 oxidation for CHF and heat-transfer-coefficient enhancement.

후 기

이 논문은 정부(교육부)의 재원으로 한국연구재단의 지원을 받아 수행된 연구임(2013M2B2 A9A03051391, 2015R1D1 A3A01018884).

REFERENCE

1. Park, S. S. and Kim, N. J., Critical Heat Flux Enhancement in Pool-boiling Heat Transfer Using Oxidized Multi-wall Carbon Nanotubes, International Journal of Energy Research, Vol. 39, No. 10, pp. 1391-1401, 2015.
2. Choi, S. U. S. and Eastman, J. A., Enhancing Thermal Conductivity of Fluids with Nanoparticles, Developments and Applications of Nano Newtonian Flows, The American Society of Mechanical Engineers Vol. 231, pp. 99-105, 1995.
3. Bang, I. C. and Chang, S. H., Boiling Heat Transfer Performance and Phenomena of Al_2O_3-water Nanofluids

from a Plain Surface in a Pool, International Journal of Heat and Mass Transfer, Vol. 48, pp. 2407-2419, 2005.

4. Park, K. J., Jung, D. S., and Shim, S. E., Nucleate Boiling Heat Transfer in Aqueous Solutions with Carbon Nanotubes Up to Critical Heat Fluxes, International Journal of Multiphase Flow Vol. 35, pp. 2593-2602, 2009.
5. Liu, Z. H. and Liao, L., Sorption and Agglutination Phenomenon of Nanofluids on a Plain Heating Surface During Pool Boiling, International Journal of Heat and Mass Transfer, Vol. 51, pp. 2593-2602, 2008.
6. Golubovic, M. N., Hettiarachchi, H. D. M., Worek, W. N., and Minkowycz, W. J., Nanofluids and Critical Heat Flux, Experimental and Analytical Study, Applied Thermal Engineering, Vol. 29, pp. 1281-1288, 2009.
7. Golubovic, M. N., Hettiarachchi, H. D. M., Worek, W. N., and Minkowycz, W. J., Nanofluids and Critical Heat Flux, Experimental and Analytical Study, Applied Thermal Engineering, Vol. 29, pp. 1281-1288, 2009.
8. Phan, H. T., Caney, N., Marty, P., Colasson, S., and Gavillet, J., Surface Wettability Control by Nanocoating: The Effects on Pool Boiling heat Transfer and Nucleation Mechanism, International Journal of Heat and Mass Transfer, Vol. 52, pp. 5459-5471, 2009.
9. Soltani, S., Etemad, S. G., and Thibault, J., Pool boiling heat transfer of non-newtonian nanofluids, International Communications in Heat and Mass Transfer, Vol. 37, pp. 29-33, 2010.
10. Truong, B., Hu, L. W., Buongiorno, J., and McKrell, T., Modification of Sandblasted Plate Heaters Using Nanofluids to Enhance Pool Boiling Critical Heat Flux, International Journal of Heat and Mass Transfer, Vol. 53, 85-94, 2010.
11. Ahn, H. S., Lee, C., Kim, H. D., and Kim, H. M., Pool Boiling CHF Enhancement by Micro/nanoscale Modification of Zircaloy-4 Surface, Nuclear Engineering and Design, Vol. 240, pp, 3350-3360, 2010.
12. Ahn, H. S., Kim, J. M., and Kim, M. H., Experimental Study of the Effect of a Reduced Graphene Oxide Coating on Critical Heat Flux Enhancement, International Journal of Heat and Mass Transfer, Vol. 60, pp. 763-771, 2013.
13. Phan, H. T., Caney, N., Marty, P., Colasson, S., and Gavillet, J., Surface Wettability Control by Nanocoating: The Effects on Pool Boiling Heat Transfer and Nucleation Mechanism, International Journal of Heat and Mass Transfer, Vol. 52, pp. 5459-5471, 2013.
14. Yu, W., Xie, H., and Wang, X., Significant Thermal Conductivity Enhancement for Nanofluids Containing Graphene Nanosheets, Physics Letters, Vol. 375, p. 1323, 2011.
15. Malayeri, M. R., Al-Janabi, A., and Müller-Steinhagen, M., Application of Nano-modified Surfaces for Fouling Mitigation," International Journal of Energy Research, Vol. 33, No. 13, pp. 1101-1113, 2009.
16. Kline, S. J., and McClintock, F. A., Describing Uncertainties in Single-sample Experiment, Mechanical Engineer, Vol. 75, pp. 3-8, 1953.